HHS Public Access

Author manuscript

Macromol Biosci. Author manuscript; available in PMC 2016 June 01.

Published in final edited form as:

Macromol Biosci. 2015 June ; 15(6): 861–874. doi:10.1002/mabi.201500013.

The effect of sterilization on silk fibroin biomaterial properties

Jelena Rnjak-Kovacina[#,1,2], **Teresa M DesRochers**[#,1,3], **Kelly A Burke**[1,4], and **David L Kaplan**[1,*]

[1] Department of Biomedical Engineering, Tufts University, Medford, MA, USA

[2] Graduate School of Biomedical Engineering, UNSW Australia, Sydney, NSW, Australia

[3] KIYATEC, Inc. Greenville, SC, USA

[4] Chemical & Biomolecular Engineering Department, University of Connecticut, Storrs, CT, USA

Abstract

The effects of common sterilization techniques on the physical and biological properties of lyophilized silk fibroin sponges is described. Sterile silk fibroin sponges were cast using a pre-sterilized silk fibroin solution under aseptic conditions or post-sterilized via autoclaving, gamma radiation, dry heat, exposure to ethylene oxide or hydrogen peroxide gas plasma. Low average molecular weight and low concentration silk fibroin solutions could be sterilized via autoclaving or filtration without significant loses of protein. However, autoclaving reduced the molecular weight distribution of the silk fibroin protein solution and silk fibroin sponges cast from autoclaved silk fibroin were significantly stiffer compared to sponges cast from unsterilized or filtered silk fibroin. When silk fibroin sponges were sterilized post-casting, autoclaving increased scaffold stiffness, while decreasing scaffold degradation rate in vitro. In contrast, gamma irradiation accelerated scaffold degradation rate. Exposure to ethylene oxide significantly decreased cell proliferation rate on silk fibroin sponges, which was rescued by leaching ethylene oxide into PBS prior to cell seeding.

[*] Corresponding author, david.kaplan@tufts.edu.

[#] Authors contributed equally to this work

Supporting Information

Supporting Information is available from the Wiley Online Library or from the author.

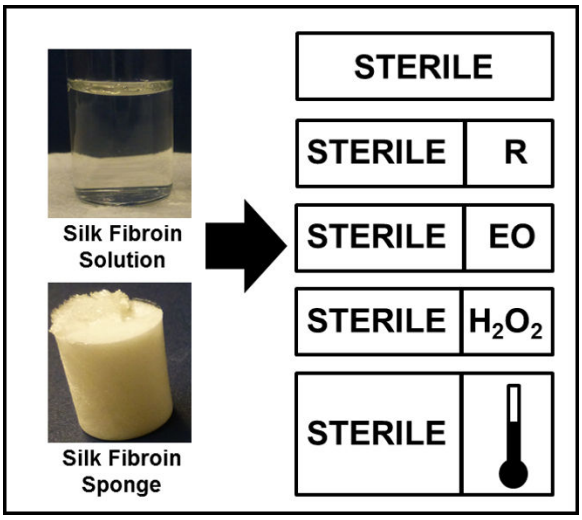

Keywords

silk fibroin; sterilization; scaffolds; biomaterial; tissue engineering

1. Introduction

Increased demand for engineered tissue constructs for use in regenerative medicine, *in vitro* disease modelling and drug testing has prompted the development of an array of biomaterials fabricated from natural and synthetic polymers, including insect [1-3] and spider silks [3-6]. In particular, a variety of material formats has been developed from *Bombyx mori* worm silk fibroin protein. *B.mori* silk fibroin has been fabricated into transparent films, microfibers, porous scaffolds, micro- and nano-particles, 3D printed structures and hydrogels. [1, 7] The protein has also been interfaced with electronics and sensors [8-9], combined with a range of synthetic [10-13] and natural polymers and biological molecules [10, 14-18] and engineered into cornea [19-21], skin [22], bone [23-26], kidney [27-30], fat [31-32], vascular [21, 33-36] and cartilage tissue equivalents. [37-38]

This progress in utility is underpinned by silk fibroin fiber processing into an aqueous silk fibroin solution that serves as source material for the various formats engineered from silk fibroin. Silk fibroin fibers are typically boiled in an alkaline solution of sodium carbonate to remove the glue-like sericin protein that coats the fibers, solubilized using a concentrated aqueous lithium bromide solution and purified by desalting via dialysis. [1, 9] The mechanical and degradation properties of silk fibroin biomaterials vary with silk fibroin fiber processing parameters (e.g., degumming time to remove the sericin), biomaterial format (e.g., film, fiber, scaffold, hydrogel) and post-processing parameters (e.g., beta-sheet (crystal) formation to obtain stability of silk fibroin biomaterials in aqueous environments, sterilization protocol). Many of these parameters have been extensively studied; for example, silk fibroin degradation can be tuned by controlling beta-sheet content of silk fibroin films.[39] Salt-leached silk fibroin scaffolds processed from aqueous (water) vs

organic (1,1,3,3,6,6-hexafluoroisopropanol (HFIP)) solvents display significantly different mechanical and degradation properties. [40]

While silk fibroin fiber processing parameters and material formats have been widely explored, the effect of sterilization on the properties of silk fibroin biomaterials is yet to be comprehensively studied. As silk fibroin biomaterials move toward large animal pre-clinical testing and clinical applications and are increasingly used in long-term *in vitro* tissue models, effective biomaterial sterilization becomes a priority. Sterilization is known to affect the physical and biological properties of many materials and biological polymers are particularly susceptible to damage from harsh sterilization protocols. [41-45]

Silk fibroin biomaterials have been sterilized by autoclaving, exposure to ethylene oxide, UV and gamma irradiation, and immersion in ethanol or methanol solutions. However, despite hundreds of manuscripts published on silk fibroin biomaterial development and use *in vitro* and *in vivo*, there are currently only a handful of reports systematically exploring the effects of sterilization techniques on silk fibroin biomaterial properties.[46-53]These studies highlight the variability of starting silk fibroin material, biomaterial formats and sterilization techniques explored, as well as use of protocols, such as immersion in ethanol, methanol or antibiotic/antimycotic solution and UV irradiation, aimed at disinfection rather than sterilization, and less likely to be appropriate in a clinical setting.

Gil and colleagues (2014) [48] studied the effects of autoclaving and immersion in 70 vol% ethanol solution on porous silk fibroin scaffolds cast via salt leaching. They found that autoclaving resulted in critical structural rearrangements of the silk fibroin, affecting degradation and mechanical properties, while 70 vol% ethanol sterilization promoted minor crystalline structure rearrangements without affecting degradation or mechanical properties. Hoffman and colleagues (2014) [51] studied the effects of autoclaving, dry heat, ethylene oxide and immersion in 70 vol% ethanol or antibiotic-antimycotic solutions on porous silk fibroin scaffold cast by salt leaching. They found that autoclaving in humid state affected scaffold porosity, while autoclaving in dry state influenced mechanical properties, and all sterilization techniques increased the variability in the physical properties of silk fibroin scaffolds. de Moraes and colleagues (2013) [46] investigated the effects of different sterilization techniques (autoclaving, UV or gamma irradiation, ethylene oxide and immersion in 70 vol% ethanol) on dense silk fibroin films and porous silk fibroin membranes made by compressed foam and lyophilization. They found that exposure to ethanol, autoclaving and ethylene oxide affected the crystallinity and mechanical properties of scaffolds and that these effects were biomaterial-type dependent. George and colleagues [47] studied the effect of sterilization by immersion in 70 vol% ethanol, autoclaving and gamma irradiation on cast silk fibroin films aimed at use in corneal tissue engineering. They found that film sterilization by autoclaving resulted in decreased film transparency and degradation rate, increased beta-sheet content and mechanical properties and changes in the surface topology of the silk fibroin films. Finally, Zhao and colleagues [53] studied the effects of different sterilization techniques on degummed silk fibroin fibers and found changes in secondary structure and mechanical properties when fibers were sterilized by autoclaving. However, this study does not directly inform biomaterial fabrication as most silk fibroin biomaterials are fabricated from reconstituted

silk fibroin solutions, rather than directly from degummed fibers. A number of reports are also available on the effects of sterilization on silk fibroin from non-*B.mori* sources, including recombinant spider silks [50, 52] and silk from hornet cocoons [49].

The goal of the present study, was to assess the effects of different sterilization techniques on the properties of lyophilized, 3D porous silk fibroin scaffolds. Lyophilized silk fibroin scaffolds are increasingly explored for soft tissue engineering applications as they offer a number of advantages over the classically used salt-leached silk fibroin scaffolds. Lyophilized silk fibroin scaffolds are fabricated by freezing an aqueous silk fibroin solution, followed by lyophilization to sublime water and thus turn ice crystals into pores. Pore size and shape is a function of the freezing rate and allows for a range of pore sizes [54]and the option of directional freezing to generate scaffolds with aligned pores.[54-55] Further, lyophilized silk fibroin scaffolds maintain structural integrity when cast from low concentration silk fibroin solution allowing for the formation of soft, sponge-like constructs. As the scaffolds are cast in the absence of salt crystals that induce beta-sheets, the final beta-sheet content and thus scaffold degradation can be controlled using the tunable water annealing process, as described for silk fibroin films. [39]

Sterile silk fibroin scaffolds may be prepared in one of two ways: either the silk fibroin solution can be sterilized followed by scaffold formation under sterile conditions or the scaffolds can be sterilized after formation. We hypothesized that the order of sterilization and scaffold formation would result in differences in the properties of the resulting scaffolds. Thus, we studied the feasibility of sterilizing the aqueous silk fibroin solution by filtration and autoclaving prior to scaffold formation, as well as the effects of five sterilization techniques (autoclaving, gamma radiation, dry heat, exposure to ethylene oxide, and hydrogen peroxide gas plasma) on preformed lyophilized silk fibroin scaffolds. Silk fibroin solution sterilization is of particular importance when post-processing sterilization is not a viable option, including for example scaffolds loaded with biological molecules that are sensitive to heat or irradiation, or for cell encapsulation in silk fibroin hydrogels. We chose techniques that are known to sterilize biological scaffolds and are compatible with clinical and regulatory settings. The aim was to identify the impact of the various methods on the structural stability, morphology, crystallinity and mechanical properties of silk fibroin scaffolds, as well as any cytotoxicity.

2. Experimental Section

2.1 Silk fibroin solution preparation

Silk fibroin solution was prepared as reported previously. [1] Briefly, pure silk fibroin was extracted from *B. mori* cocoons by degumming the fibers in a 0.02 M boiling sodium carbonate solution (Sigma-Aldrich, St. Louis, MO) for 5, 10, 30 or 60 min to remove sericin. Adequate sericin removal using short degumming times has been previously demonstrated. [56] Dried silk fibroin fibers were solubilized in 9.3 M aqueous lithium bromide (Sigma-Aldrich, St. Louis, MO) for 4 h at 60°C. 5 and 10 min degummed silk fibroin fibers were dissolved in the lithium bromide solution at 20 wt%, while 30 and 60 min degummed fibers were dissolved at 25 wt%. The solution was dialyzed using D-Tube™ Dialyzers (3500 MWCO, EMD Millipore, Billerica, MA) against deionized water. The

concentration of the silk fibroin solution was determined by drying a known volume of the solution and massing the remaining solids. This protocol resulted in a 6–8 wt% silk fibroin solution. Silk fibroin solutions were stored at 4°C.

2.2 Sterilization of liquid silk fibroin solution

Silk fibroin solutions were diluted to 0.5-4 wt% in deionized water and sterilized by filtration through a 0.22 μm Millex GP PES membrane syringe-driven filter unit (Millipore, Billerica, MA) using 5 ml plastic syringes and 2 ml silk fibroin solution/test or by autoclaving at 121°C for 20 min under a high pressure saturated steam cycle (3 ml/test in 10 ml glass vials covered with aluminum foil).

2.3 Characterization of sterilized silk fibroin solutions

Absorbance spectra of silk fibroin solutions prior to and following autoclaving were obtained between 300 nm and 750 nm at 10 nm intervals using a plate reader (SpectraMax M2, Molecular Devices, Sunnyvale, CA). Differences in the molecular weight (MW) distribution of silk fibroin molecules resulting from different sterilization techniques were visualized with sodium dodecyl sulfate polyacrylamide gel electrophoresis (SDS-PAGE). For each sample, 50 μg of solubilized silk fibroin protein was loaded into a 3–8 wt% Tris Acetate Novex gel (NuPAGE, Invitrogen, Carlsbad, CA) under reducing conditions. The gel was run at 200 V for 45 min with a high molecular weight ladder (HiMark Unstained, Invitrogen) and then stained with a Colloidal Blue staining kit (Invitrogen). Protein distribution was imaged using a GBox XR5 gel imager (Syngene, Frederick MD) and quantified by taking densitometric measurements along the length of the gel (ImageJ, NIH, Bethesda, MD) as previously described. [56]

2.4 Preparation of silk fibroin scaffolds

A 4 wt% aqueous silk fibroin solution in deionized water was dispensed into wells of standard 24-well cell culture plates (3 ml/well), frozen overnight at −20°C in a standard laboratory freezer and lyophilized at −80°C for 48 h. Dry scaffolds were removed from the molds and rendered insoluble in aqueous environments by water annealing (exposure to water vapor under partial vacuum) for 18 h at room temperature to induce β-sheet formation. [39]

2.5 Sterilization of silk fibroin scaffolds

Dry silk fibroin scaffolds were sterilized by autoclaving, gamma irradiation, dry heat, ethylene oxide, or hydrogen peroxide gas plasma prior to further analyses. Autoclaving: Scaffolds were wrapped individually in aluminum foil pouches and autoclaved at 121°C for 20 min under a high pressure saturated steam cycle (Sanyo/Panasonic MLS-3871L autoclave). Gamma irradiation: Scaffolds were placed in plastic tubes and exposed to 166 Gy/min from a Cobalt-60 isotope source over a 2-3 hour period to a total of 15 kGy. Dry heat: A glass petri dish containing silk fibroin scaffolds was placed inside a pre-heated oven (Fisher Scientific Isotemp Vacuum Oven Model 281A, at atmospheric pressure) at 160°C. Once the temperature in the middle of the scaffolds reached 160°C (determined using a thermocouple and Omega HH21A microprocessor thermometer placed in the middle of a

scaffold in a separate Petri dish), scaffolds were sterilized for 20 min at 160-163°C. Ethylene oxide: Scaffolds were placed in sterilization pouches and exposed to ethylene oxide gas for 10 h, followed by 2 h degassing in the sterilizer chamber and additional 24 h degassing in a vacuum oven at room temperature to remove residual ethylene oxide. Hydrogen peroxide gas plasma: Scaffolds were placed in sterilization pouches and exposed to hydrogen peroxide gas plasma using the STERRAD Sterilization System (ASP, Irvine, CA). Following sterilization scaffolds were rehydrated in water under sterile conditions and trimmed to appropriate dimensions for further testing using razor blades and biopsy punches.

2.6 Characterization of the physical properties of sterilized silk fibroin scaffolds

Swelling—The mass of silk fibroin scaffolds (12 mm × 2 mm height) in dry state, hydrated in water or PBS was recorded. Swelling was expressed as fold increase in mass when hydrated in water or PBS compared to dry state.

Scaffold morphology—Scaffolds were visualized by scanning electron microscopy (SEM). Scaffolds were dehydrated in increasing concentrations of ethanol and dried overnight in hexamethyldisilazane. Dried samples were sputter coated with platinum/palladium (40 mA, 60 seconds) and imaged with a field emission SEM and 5 kV electron beam (Supra55VP, Zeiss, Oberkochen, Germany).

Scaffold crystallinity (β-sheet content)—Fourier transform infrared spectroscopy (FTIR) analysis was performed to quantify the beta-sheet content of scaffold sterilized under different conditions. Analyses were performed using an FT/IR-6200 Spectrometer (Jasco, Easton, MD), equipped with a triglycine sulfate detector in attenuated total reflection (ATR) mode. For each measurement, 64 scans were co-added with resolution 4 cm^{-1}, and the wave numbers ranged from 600-4000 cm^{-1}. The background spectra were collected under the same conditions and subtracted from the scan for each sample. Fourier self-deconvolution (FSD) of the infrared spectra covering the Amide I region (1595~1705 cm^{-1}) was performed with Opus 5.0 software (Bruker Optics Corp., Billerica MA), as described previously.[57] The deconvolved Amide I spectra were area-normalized, and the relative areas of the single bands were used to determine the fraction of the secondary structural elements in scaffolds.

Scaffold sterility—Each scaffold (12 mm × 2 mm height) was placed in 3 ml of Luria broth (Sigma-Aldrich, St. Louis, MO) and incubated in a shaker at 37°C for 48 h. 100 μl of Luria broth was removed from each sample and absorbance at 600 nm was recorded using a SpectraMax plate reader (Molecular Devices, Sunnyvale, CA).

Mechanical properties—Compressive mechanical properties of hydrated (PBS, pH 7.4, 37°C) samples (6 mm Ø × 3 mm height) were obtained using an Instron 3366 testing frame equipped with a 100 N load cell as previously described. [58]

Scaffold degradation— *In vitro* degradation of scaffolds was analyzed as previously described. [49] Briefly, scaffolds (12 mm Ø × 2 mm height) were placed in pre-weighted 1.5 ml plastic microcentrifuge tubes and dried at 60°C. The mass of dry scaffolds was recorded

and 1 ml of 1 U/ml Protease XIV solution in PBS (Sigma-Aldrich, St. Louis, MO) was added to each tube and incubated at 37°C. Every 2 days, Protease XIV was removed, samples were washed twice with deionized water, dried at 60°C and dry mass was recorded prior to addition of fresh Protease XIV solution. Scaffold degradation was calculated as percent remaining mass compared to original scaffold mass. Control samples were incubated in PBS to baseline silk fibroin sponge degradation in the absence of Protease XIV.

2.7 Characterization of the biological properties of sterilized silk fibroin scaffolds

Human foreskin fibroblasts were a generous gift from Dr. Jonathan Garlick and maintained in Dulbecco's Modified Eagle's Medium (DMEM, high glucose) supplemented with 10 wt % fetal bovine serum and penicillin/streptomycin (Life Technologies, Grand Island, NY) at 37°C, 5% CO_2.

Scaffolds (12 mm Ø, 2 mm height) were incubated in cell culture medium for 1 h prior to cell seeding. Excess media was aspirated from the scaffolds to ensure pore void volume was accessible to cells and cells were seeded at 2×10^5 cells per scaffolds ($1x10^5$ cells in 90 μl media on each scaffold surface). Cell-laden scaffolds were incubated for 3h at 37°C, 5% CO_2. At 3 h post-seeding, scaffolds were washed with PBS and cell attachment analyzed by Alamar blue (Invitrogen, Carlsbad, CA). One ml of Alamar blue reagent working solution (10 vol% in in cell culture media) was added per scaffold and incubated at 37°C, 5% CO_2 for 2 h. Following incubation, aliquots (100 μL) were transferred to black 96-well plates and quantified for fluorescence intensity with a fluorescence plate reader using an excitation wavelength of 550 nm and an emission wavelength of 590 nm. Scaffolds were washed with PBS and incubated in cell culture media at 37°C, 5% CO_2 for 10 days. Alamar blue assay was repeated at days 1, 5 and 10 post-seeding. Acellular scaffolds and tissue culture wells were also maintained in culture medium as above and were analyzed similarly as blank controls to adjust for background fluorescence. All cell attachment and proliferation values are expressed relative to Alamar blue readings of tissue culture plastic wells seeded in the same manner.

2.8 Statistical analyses

Data are expressed as mean ± standard deviation (SD). Statistically significant differences were determined by one- or two-way analysis of variance (ANOVA) and the Tukey post-test. Statistical significance was accepted at $p<0.05$ and indicated in the figures as *$p<0.05$, **$p<0.01$, ***$p<0.001$ and ****$p<0.0001$.

3. Results and Discussion

Sterilization protocols are known to affect the physical and biological properties of both natural and synthetic polymers and have been shown to be material format and sterilization protocol dependent. [41-47, 51]While a range of methodologies have been established to control and tune the physical and biological properties of *B. mori* silk fibroin biomaterials, the effect of subsequent sterilization processes on the biomaterial properties, and in particular lyophilized silk fibroin sponges, remains largely underexplored.

The current study investigated the feasibility and effects of different sterilization techniques on silk fibroin sponges, by either casting sponges under sterile conditions using pre-sterilized silk fibroin solution or sterilizing sponges post-casting. The study findings, as well as advantages and disadvantages of each sterilization technique, are summarized in **Table 1**. To the best of our knowledge, this is the first systematic investigation of the effects of sterilization protocols on silk fibroin solutions and lyophilized silk fibroin sponges.

3.1 Sterilization of Liquid Silk Fibroin Solution

Two different techniques for sterilizing liquid silk fibroin were examined, filtration through a 0.22 μm filter and autoclaving. Both methodologies are readily available in laboratories and hospitals and are routinely used to sterilize medical grade reagents and equipment. One of the critical steps in the formation of aqueous silk fibroin solutions is the amount of time the fibers from the *B.mori* silk worm cocoon are boiled in the sodium carbonate solution during the sericin removal step. Longer boiling time correlates with smaller average molecular weight distribution of silk fibroin molecules and this property can be utilized to tailor physical properties of silk fibroin biomaterials[56]. Therefore, for the examination of sterile filtration and autoclaving of the liquid silk fibroin solution a number of different silk fibroin boil times (5, 10, 15, 30, 45, and 60 minutes) at four different concentrations of silk fibroin protein (0.5, 1, 2, and 4 wt%) were explored. The overall viscosity of the solutions was observed to decrease with boiling time and to increase with silk fibroin concentration. Thus, the most viscous solution was the 5-min boiling at 4 wt% and the least viscous was the 60-min boiling at 0.5 wt%. While silk fibroin is often used at much higher concentrations (6-18 wt%) to generate constructs aimed at bone tissue engineering and regeneration, lyophilized silk fibroin sponges are much better suited to engineering soft tissues and not likely to be cast at high silk fibroin concentrations.

The feasibility of sterile filtration of all the different silk fibroin solutions was examined first. The filtration process was limited by the strength the user could exert upon the syringe-driven filter unit and the capacity of the filter membrane prior to clogging. Therefore, the amount of solution recovered after sterile filtration was initially examined (**Table 2**). 2 mL of silk fibroin solution was filtered through a 0.22 μm filter and the volume of the filtrate was measured and expressed as a percentage of the initial volume. The 5-min boiling solution was resistant to sterile filtration at all concentrations, and the ability to pass the silk fibroin solution through the syringe increased with increasing boiling time. Silk fibroin concentration also played a factor in the ability to sterilize the solution with filtration as recovery decreased with concentration of silk fibroin. 45-min and 60-min boiling were 100% recoverable at concentrations below 4 wt%, so they were only examined closely at 4 wt%. Thus, based upon recovery rates, it is only efficient to filter sterilize silk fibroin solutions that have been boiled for at least 30 minutes, where the majority of protein species were around 150 kDa (**Supplementary Figure 1** and[56]). It is possible that even though liquid passed through the filters, the silk fibroin protein was trapped on the silk fibroin membrane, resulting in the more dilute filtrate. Therefore, the resulting silk fibroin concentration post-filtration was also examined (**Table 3**). It was evident that the liquid silk fibroin protein was trapped on the filters for the 10-min and 15-min boiling, as the final silk fibroin concentration in the filtrate was 39.7±33.5% and 89.0±19.0% of the original

concentration respectively. However, the liquid that passed through the filters at 30-min and greater boiling retained the original concentration of silk fibroin within the solution. Aside from recovery of solution and retention of the starting silk fibroin concentrations, the appearance of the silk fibroin solution before and after filtration was also examined (**Figure 1A**). The solutions were clearer post filtration than they were prior to filtration. This may be caused by the removal of some of silk fibroin aggregates from the solution (in particular silk fibroin that adopted crystalline secondary structure), or it may reflect the removal of other contaminating components that were not sufficiently removed during the preparation from silk fibroin worm cocoons. Finally, the size distribution of the recovered proteins within the filter sterilized silk fibroin solutions was examined via SDS-PAGE and Coomassie staining (**Figure 1E**). Only the 30-min, 45-min, and 60-min boiling 4 wt% solutions were examined in this manner. The gel reflects the broad molecular weight distribution of silk fibroin protein species following degumming and a decrease in the average silk fibroin protein molecular weight with increasing boiling times (**Supplementary Figure 1**) as the overall smeared signal shifts lower on the gel in the 60-min boiling compared to the 30-min boiling, but no obvious effect of silk fibroin filtration on the molecular weight distribution was observed (**Figure 1E-F**). Filtration was thus a feasible methodology for sterilizing low average molecular weight, low concentration silk fibroin solutions. Such solutions are often suitable for soft tissue engineering (e.g., adipose and neural tissues), both for casting lyophilized silk fibroin sponges (Rnjak-Kovacina et al., submitted) and silk fibroin hydrogels. [59]

Autoclaving the silk fibroin solution prior to biomaterial casting is often reported in the literature, but with little information on the effects of this process on the silk fibroin protein. Sterilization of the liquid silk fibroin solutions via autoclaving revealed that there was a change in the appearance of the solutions (**Figure 1B**). While the 5-min and 10-min boiling did not appear to change, the 15-min, 30-min, 45-min, and 60-min boiling became more opaque with autoclaving. This visual change was associated with a shift in absorbance spectrum (**Figure 1C**) likely due to an increase in protein aggregation as reflected by the significant increase in absorbance at 350 nm upon autoclave sterilization (**Figure 1D**). Thus, the size distribution of protein before and after autoclaving was examined by SDS-PAGE followed by Coomassie staining (**Figure 1E**). Autoclaving the silk fibroin solution appeared to compound the boiling effect upon protein size. While sterile filtration resulted in protein sizes similar to the unsterilized silk fibroin solution, autoclaving resulted in a decrease in average molecular weight. This was particularly obvious in short boiling times (5-15 min), where an increase in lower molecular weight species was observed following autoclaving (**Figure 1E-F**).

To demonstrate the feasibility of using sterilized silk fibroin solutions to cast lyophilized silk fibroin sponges, a set of protocols was developed to cast the sponges under sterile conditions. Silk fibroin sponges were cast from pre-sterilized silk fibroin solutions in sterile 24-well tissue culture plates in a laminar flow hood. Following freezing, scaffolds were placed in sterile autoclave bags and lyophilized. Scaffolds were water annealed in a glass desiccator which was sterilized by autoclaving and placed inside a laminar flow hood.

Finally, the mechanical properties of the silk fibroin scaffolds formed from 30-min boiling, 4 wt% silk fibroin solution that had been either sterile filtered or autoclaved were examined. This boil time and concentration was chosen as it is the commonly used to make silk fibroin scaffolds for tissue engineering applications. [54] Scaffolds were compressed under unconfined conditions using a 100 N load cell at physiological temperature and pH (37°C, PBS). No difference in the shape of the strain-strain curve or compressive modulus was observed in scaffolds formed from filtered compared to unsterilized silk fibroin, but autoclaved silk fibroin resulted in significantly stiffer scaffolds compared to those formed from unsterilized or filter sterilized silk fibroin (**Figure 2**). Lower average molecular weight was expected to correlate with lower stiffness and strength, thus it is possible that an increase in β-sheet content in the silk fibroin solution following autoclaving was responsible for these unexpected bulk material properties. Higher crystallinity has been shown to correlate with increased silk fibroin biomaterial stiffness. [39] This is consistent with the findings by George and colleagues (2013) [47], who demonstrated that despite a shift in the protein size distribution toward lower molecular weight species, steam sterilization of pre-cast silk fibroin films resulted in increased material stiffness and strength, correlated with increased β-sheet content.

3.2 Sterilization of Silk fibroin Scaffolds

The feasibility of casting sterile silk fibroin sponges from pre-sterilized silk fibroin solutions was demonstrated, however, the successful and cost-effective manufacture of silk fibroin-based medical devices and biomaterials will likely involve scaffold sterilization post-casting. Therefore, the effects of thermal (autoclaving and dry heat), physical (gamma irradiation) and chemical (ethylene oxide and hydrogen peroxide plasma) sterilization protocols on the physical and biological properties of silk fibroin sponges were explored. Thermal sterilization protocols, in particular steam sterilization via autoclaving, are routinely used to sterilize medical devices made from metallic alloys, but are generally unsuitable for biomedical polymers and in particular proteins, causing major changes in mechanical and degradation properties. [60] However, due to the unique mechanical and stability properties of silk fibroin, autoclaving has been routinely used to sterilize silk fibroin-based biomaterials, maximizing the β-sheet content and thus the stiffness and strength. [39] Gamma irradiation is a routinely used sterilization protocol for a range of medical devices and biological molecules, resulting in sterilization via oxidation of biological tissue. [60] However, it has been demonstrated to affect the physical properties of a number of synthetic and natural polymers, resulting in changes in molecular weight distribution, degradation and mechanical properties. [60] Chemical sterilization protocols are often employed as an alternative to thermal sterilization for materials that cannot withstand high temperatures. [60] Ethylene oxide has, for many years, been the alternative sterilization method of choice as it is bactericidal, sporicidal and virucidal via alkylation of a number of chemical groups in the nucleic acids of microbes, causing cell injury and death. However, ethylene oxide toxicity and suspected carcinogenicity make the risk of ethylene oxide retention in the sterilized material problematic and cause safety and environmental concerns in the facilities operating the sterilizer. [60] Gas plasma using hydrogen peroxide has emerged as an alternative to ethylene oxide in many hospital and research settings, with less risk of severe or chronic toxicity compared to ethylene oxide.

In order to examine the effects of sterilization on properties of silk fibroin scaffolds, scaffolds were cast from a 30-min boiling, 4 wt% silk fibroin solution and beta-sheet formation was induced by water annealing to stabilize the scaffolds in aqueous conditions. We chose this boiling time and silk fibroin concentration as they are typically used for tissue engineering purposes in our laboratory. For all studies, silk fibroin scaffolds that were not sterilized were used as controls.

The physical characteristics of the scaffolds, including their swelling properties (**Figure 3A**), morphology (**Figure 3B)** and crystallinity (**Figure 3C**) were examined. While there was a trend for the autoclaved scaffolds to swell less in water or PBS, there was no significant difference in swelling properties among the different sterilization techniques. Additionally, there was no obvious difference in pore size or morphology observed by SEM. FTIR spectra of the silk fibroin sponges showed characteristic peaks (amide I at 1701 and 1623 cm^{-1}, amide II at 1520 cm^{-1} and amide III at 1265 cm^{-1}) and no shifts in the spectra following sterilization (**Supplementary Figure 2**). There were small, but not significant changes observed in the overall β-sheet content of silk fibroin sponges sterilized by different techniques (**Figure 3C**). Finally, successful sterilization of scaffolds by all sterilization techniques was confirmed by incubating them in LB broth for 48 h and measuring the absorbance at 600 nm to assess bacterial growth (**Figure 3D**). Bacterial growth was only observed in the non-sterilized samples. The most commonly validated gamma irradiation dose for medical devices is 25 kGy, but much work has been invested into establishing lower doses that result in sterility while minimizing negative physical effects. We tested a 15 kGy irradiation dose on the silk fibroin scaffolds. While no bacteria growth in LB broth containing these scaffolds over 48 h was observed, we acknowledge the need for more rigorous testing of this sterilization dose to establish scaffold sterility.

The mechanical properties of the sterilized silk fibroin scaffolds were examined. Scaffolds were compressed under unconfined conditions using a 100 N load cell at physiological temperature and pH (37°C, PBS). All scaffolds were compressed to 80% strain. The strain-strain curves (**Figure 4A**) demonstrated that more force was required to compress autoclaved and plasma treated scaffolds to 80% strain, compared to other conditions. Autoclaved samples also demonstrated significantly higher compressive modulus compared to non-sterilized samples ($p<0.0001$), as well as compared to all other sterilization techniques ($p<0.01$ compared to plasma-treated and $p<0.001$ compared to all other sterilization methods) (**Figure 4B**).

As the tunability of silk fibroin scaffold degradation through the control of β-sheet content is frequently exploited for silk fibroin, the effect of sterilization on the degradation of the silk fibroin scaffolds by protease XIV was examined. Water annealed silk fibroin scaffolds did not degrade significantly in PBS over an eight day period (**Figure 4C**), while scaffolds exposed to protease XIV degraded and thus were reduced in mass over time (**Figure 4D**). The autoclaved scaffolds were the most resistant to degradation, with significantly lower loss in mass compared to non-sterilized scaffolds at every time point ($p<0.001$) while the gamma irradiated were the fastest to degrade, with significantly lower ($p<0.05$) mass compared to non-sterilized scaffolds at day 6. The other sterilized scaffolds all remained similar to non-sterile scaffolds in the extent of degradation over time. The changes in silk

fibroin following autoclaving are likely a result of changes in the amorphous regions of silk fibroin. Similar observations were made by Gil and colleagues (2014) with porous silk fibroin scaffolds generated by leaching salt from aqueous or organic silk fibroin solutions. [48] There, the authors demonstrated that autoclaving promoted greater restriction in the inter- and intra-molecular interactions in the amorphous regions of the silk fibroin chain network, thus affecting mechanical properties and degradation of silk fibroin scaffolds, independent of β-sheet content. [48] The accelerated rate of degradation in gamma irradiated silk fibroin scaffolds is likely a result of protein damage caused by gamma rays. Gamma rays ionise water molecules in their trajectory, rupturing chemical bonds and thereby releasing radiation products in the form of H+ and OH−. These radiation products are responsible for the vast majority of damage to proteins during the irradiation process. [61] This damage may be reduced by performing gamma irradiation under cold conditions or in the presence of free radicals scavengers, such as ascorbic acid. [61]

Finally, the ability of silk fibroin scaffolds sterilized under different conditions to support cell attachment and proliferation was examined using human foreskin fibroblasts. In these studies the non-sterilized group was omitted, as cells could not be cultured on non-sterile scaffolds for prolonged periods of time due to rapid contamination. Cells were seeded onto five scaffolds of each sterilization type and three additional scaffolds without cells were used as background controls. After 3 h, each scaffold was washed with PBS to remove any non-adherent cells and relative cell adhesion was determined using the Alamar blue cell assay **(Figure 5A).** Results are expressed as fluorescence signal relative to that on tissue culture plastic (TCP) with the same number of cells seeded. The ethylene oxide sterilized scaffolds had a significant reduction in the amount of cells initially attaching compared to the plasma sterilized scaffolds. Alamar Blue readings were repeated at 1, 5, and 10 days post seeding (**Figure 5B**). All sterilization techniques resulted in similar numbers of cells at day 10 post-seeding. However, the autoclaved samples promoted proliferation at a faster rate than the other sterilization techniques (attributed to differences in the mechanical properties of autoclaved samples), and cell proliferation on ethylene oxide-treated scaffolds remained the slowest throughout the experiment. This was likely a result of residual toxic ethylene oxide products in the scaffold, even after extensive degassing. Of note was also the initial drop in cell proliferation within 24 h for the plasma-sterilized scaffolds. Thus, we examined how incubating the scaffolds for 24 or 48 h in PBS to leach out potential cytotoxic compounds prior to cell seeding would affect cell attachment and/or proliferation (**Figures 5C&D**). Pre-leaching the ethylene oxide sterilized scaffolds for either 24 or 48 h had a significant impact upon both cell attachment and cell proliferation with little to no significant difference between the two time points (**Figure 5C**). While a more in-depth analysis of ethylene oxide leaching over time is required to establish when scaffolds are ethylene oxide free, a methodology that requires significant leaching in sterile PBS solutions prior to material implantation or cell seeding is not likely to be feasible in hospital settings. Pre-leaching the H_2O_2 gas plasma sterilized scaffolds prior to cell seeding did not have a significant impact upon cell attachment or proliferation, but the initial drop in cell proliferation in the unleached H_2O_2 gas plasma sterilized scaffolds was eradicated by leaching the scaffolds for either 24 or 48 h (**Figure 5D**).

4. Conclusion

Sterilization of silk fibroin solutions prior to silk fibroin sponge casting is a feasible, but not practical means of generating sterile silk fibroin biomaterials. However, some applications (eg. casting of silk sponges in plastic bioreactor systems) may require pre-sterilization of silk fibroin solutions prior to sponge casting. Sterilization of silk solutions is also essential for cell encapsulation in silk hydrogels. For these applications, filtration is limited to low average molecular weight, low concentration solutions and does not affect the mechanical properties of final biomaterials while autoclaving can be performed on all silk fibroin solutions, but affects the molecular weight distribution of the silk fibroin proteins, as well as the mechanical properties of the final silk fibroin biomaterial. Post-sterilization of silk fibroin sponges is simpler and less time consuming than pre-sterilization due to the number of steps that may be performed under non-sterile conditions. Autoclaving is a simple and readily available sterilization technique for lyophilized silk fibroin sponges, but it increases the stiffness and decreases the degradation rate of silk fibroin sponges. Gamma irradiation accelerated scaffold degradation, but no other obvious physical changes were observed with any sterilization technique. Ethylene oxide reduced cell binding and proliferation likely due to leaching of toxic byproducts from the scaffolds while autoclaving improved cell proliferation over a 10 day period. Thus, while a number of techniques are available for sterilizing silk fibroin scaffolds, the final choice will depend on the intended use and thus material properties that are of importance. This study defined the effects of common sterilization techniques on the physical and biological properties of lyophilized silk fibroin sponges, thus allowing for a more informed choice of sterilization techniques for different purposes.

Supplementary Material

Refer to Web version on PubMed Central for supplementary material.

Acknowledgments

Acknowledgments: We thank the NIH (NIH P41 EB002520; EY020856; F32-DK093194 awarded to KAB) and the Air Force Office of Scientific Research for support. We thank Hannah Baker and Dr. George Christ (WFIRM) for their assistance with gamma sterilization, Dr. Michael House and staff at Tufts Medical for their assistance with plasma sterilization, Dr. Chiara Ghezzi for her advice on mechanical testing and Carmen Preda for technical assistance.

References

1. Rockwood DN, Preda RC, Yucel T, Wang XQ, Lovett ML, Kaplan DL. Nat. Protoc. 2011; 6:1612. [PubMed: 21959241]
2. Sutherland TD, Young JH, Weisman S, Hayashi CY, Merritt DJ. Annu. Rev. Entomol. 2010; 55:171. [PubMed: 19728833]
3. Hardy JG, Scheibel TR. Prog. Polym. Sci. 2010; 35:1093.
4. Lewis RV. Chem. Rev. 2006; 106:3762. [PubMed: 16967919]
5. Shao ZZ, Vollrath F. Nature. 2002; 418:741. [PubMed: 12181556]
6. Vollrath F. J. Biotechnol. 2000; 74:67. [PubMed: 11763504]
7. Pritchard EM, Kaplan DL. Expert. Opin. Drug. Del. 2011; 8:797.

8. Kim DH, Viventi J, Amsden JJ, Xiao JL, Vigeland L, Kim YS, Blanco JA, Panilaitis B, Frechette ES, Contreras D, Kaplan DL, Omenetto FG, Huang YG, Hwang KC, Zakin MR, Litt B, Rogers JA. Nat. Mater. 2010; 9:511. [PubMed: 20400953]
9. Tao H, Kaplan DL, Omenetto FG. Adv. Mater. 2012; 24:2824. [PubMed: 22553118]
10. Lee KY, Ha WS. Polymer. 1999; 40:4131.
11. Li MZ, Lu SZ, Wu ZY, Tan K, Minoura N, Kuga S. Int. J. Biol Macromol. 2002; 30:89. [PubMed: 11911898]
12. Liu Y, Shao ZZ, Zhou P, Chen X. Polymer. 2004; 45:7705.
13. Yoo MK, Kweon HY, Lee KG, Lee HC, Cho CS. Int. J. Biol. Macromol. 2004; 34:263. [PubMed: 15374683]
14. Hu X, Park SH, Gil ES, Xia XX, Weiss AS, Kaplan DL. Biomaterials. 2011; 32:8979. [PubMed: 21872326]
15. Hu X, Tang-Schomer MD, Huang WW, Xia XX, Weiss AS, Kaplan DL. Adv. Funct. Mater. 2013; 23:3875. [PubMed: 25093018]
16. Hu XA, Wang XL, Rnjak J, Weiss AS, Kaplan DL. Biomaterials. 2010; 31:8121. [PubMed: 20674969]
17. Marsano E, Corsini P, Canetti M, Freddi G. Int. J. Biol. Macromol. 2008; 43:106. [PubMed: 18513793]
18. Yeo IS, Oh JE, Jeong L, Lee TS, Lee SJ, Park WH, Min BM. Biomacromolecules. 2008; 9:1106. [PubMed: 18327908]
19. Gil ES, Mandal BB, Park SH, Marchant JK, Omenetto FG, Kaplan DL. Biomaterials. 2010; 31:8953. [PubMed: 20801503]
20. Lawrence BD, Marchant JK, Pindrus MA, Omenetto FG, Kaplan DL. Biomaterials. 2009; 30:1299. [PubMed: 19059642]
21. Wu J, Rnjak-Kovacina J, Du YQ, Funderburgh ML, Kaplan DL, Funderburgh JL. Biomaterials. 2014; 35:3744. [PubMed: 24503156]
22. Bellas E, Seiberg M, Garlick J, Kaplan DL. Macromol.biosci. 2012; 12:1627. [PubMed: 23161763]
23. Correia C, Bhumiratana S, Yan LP, Oliveira AL, Gimble JM, Rockwood D, Kaplan DL, Sousa RA, Reis RL, Vunjak-Novakovic G. Acta biomaterialia. 2012; 8:2483. [PubMed: 22421311]
24. Hofmann S, Hilbe M, Fajardo RJ, Hagenmuller H, Nuss K, Arras M, Muller R, von Rechenberg B, Kaplan DL, Merkle HP, Meinel L. Eur. J. Pharm. Biopharm. 2013; 85:119. [PubMed: 23958323]
25. Kim HJ, Kim UJ, Kim HS, Li CM, Wada M, Leisk GG, Kaplan DL. Bone. 2008; 42:1226. [PubMed: 18387349]
26. Mandal BB, Grinberg A, Gil ES, Panilaitis B, Kaplan DL. P. Natl. Acad. Sci. USA. 2012; 109:7699.
27. DesRochers TM, Ko W, Subramanian B, Perrone R, Shah JV, Kaplan DL. J. Tissue. Eng. Regen. Med. 2012; 6:126.
28. DesRochers TM, Palma E, Kaplan DL. Adv. Drug. Deliver. Rev. 2014; 69:67.
29. DesRochers TM, Suter L, Roth A, Kaplan DL. PloS One. 2013:8.
30. Subramanian B, Rudym D, Cannizzaro C, Perrone R, Zhou J, Kaplan DL. Tissue Eng. Part A. 2010; 16:2821. [PubMed: 20486787]
31. Bellas E, Panilaitis BJB, Glettig DL, Kirker-Head CA, Yoo JJ, Marra KG, Rubin JP, Kaplan DL. Biomaterials. 2013; 34:2960. [PubMed: 23374707]
32. Choi JH, Bellas E, Vunjak-Novakovic G, Kaplan DL. Methods. Mol. Biol. 2011; 702:319. [PubMed: 21082412]
33. Lovett M, Cannizzaro C, Daheron L, Messmer B, Vunjak-Novakovic G, Kaplan DL. Biomaterials. 2007; 28:5271. [PubMed: 17727944]
34. Rnjak-Kovacina J, Wray LS, Golinski JM, Kaplan DL. Adv. Funct. Mater. 2014; 24:2188. [PubMed: 25395920]
35. Seib FP, Herklotz M, Burke KA, Maitz MF, Werner C, Kaplan DL. Biomaterials. 2014; 35:83. [PubMed: 24099708]

36. Soffer L, Wang XY, Zhang XH, Kluge J, Dorfmann L, Kaplan DL, Leisk G. J. Biomat. Sci. Polym. Ed. 2008; 19:653.
37. Chao PHG, Yodmuang S, Wang XQ, Sun L, Kaplan DL, Vunjak-Novakovic G. J. Biomed. Mater. Res. B. 2010; 95B:84.
38. Wang YZ, Blasioli DJ, Kim HJ, Kim HS, Kaplan DL. Biomaterials. 2006; 27:4434. [PubMed: 16677707]
39. Hu X, Shmelev K, Sun L, Gil ES, Park SH, Cebe P, Kaplan DL. Biomacromolecules. 2011; 12:1686. [PubMed: 21425769]
40. Wang Y, Rudym DD, Walsh A, Abrahamsen L, Kim HJ, Kim HS, Kirker-Head C, Kaplan DL. Biomaterials. 2008; 29:3415. [PubMed: 18502501]
41. Faraj KA, Brouwer KM, Geutjes PJ, Versteeg EM, Wismans RG, Deprest JA, Chajra H, Tiemessen DM, Feitz WFJ, Oosterwijk E, Daamen WF, Kuppevelt TH. Tissue. Eng. Regen. Med. 2011; 8:460.
42. Lim LY, Khor E, Kool O. J. Biomed. Mater. Res. B. Appl. Biomater. 1998; 43:282.
43. Shearer H, Ellis MJ, Perera SP, Chaudhuri JB. Tissue Eng. 2006; 12:2717. [PubMed: 17518641]
44. Vink P, Pleijsier K. Biomaterials. 1986; 7:225. [PubMed: 3719042]
45. Wiegand C, Abel M, Ruth P, Wilhelms T, Schulze D, Norgauer J, Hipler UC. J. Biomed. Mater. Res. B. Appl. Biomater. 2009; 90B:710. [PubMed: 19213054]
46. de Moraes MA, Weska RF, Beppu MM. J. Biomed. Mater. Res. B. Appl. Biomater. 2013 DOI: 10.1002/jbm.b.33069.
47. George KA, Shadforth AM, Chirila TV, Laurent MJ, Stephenson SA, Edwards GA, Madden PW, Hutmacher DW, Harkin DG. Mater. Sci. Eng. C. Mater. Biol. Appl. 2013; 33:668. [PubMed: 25427472]
48. Gil ES, Park SH, Hu X, Cebe P, Kaplan DL. Macromol. Biosci. 2014; 14:257. [PubMed: 24519787]
49. Hattori S, Terada D, Bintang AB, Honda T, Yoshikawa C, Teramoto H, Kameda T, Tamada Y, Kobayashi H. Bioinsp.Biomim. Nanomater. 2012; 1:195.
50. Hedhammar M, Bramfeldt H, Baris T, Widhe M, Askarieh G, Nordling K, von Aulock S, Johansson J. Biomacromolecules. 2010; 11:953. [PubMed: 20235574]
51. Hofmann S, Stok KS, Kohler T, Meinel AJ, Muller R. Acta Biomater. 2014; 10:308. [PubMed: 24013025]
52. Lucke M, Winter G, Engert J. Int. J. Pharm. 2015; 481:125. [PubMed: 25596418]
53. Zhao Y, Yan X, Ding F, Yang Y, Gu X. J. Biomed. Sci. Eng. 2011; 4:397.
54. Wray LS, Rnjak-Kovacina J, Mandal BB, Schmidt DF, Gil ES, Kaplan DL. Biomaterials. 2012; 33:9214. [PubMed: 23036961]
55. Mandal BB, Gil ES, Panilaitis B, Kaplan DL. Macromol. Biosci. 2013; 13:48. [PubMed: 23161731]
56. Wray LS, Hu X, Gallego J, Georgakoudi I, Omenetto FG, Schmidt D, Kaplan DL. J. Biomed. Mater. Res. B. Appl. Biomater. 2011; 99B:89. [PubMed: 21695778]
57. Hu X, Kaplan D, Cebe P. Macromolecules. 2006; 39:6161.
58. Gil ES, Kluge JA, Rockwood DN, Rajkhowa R, Wang LJ, Wang XG, Kaplan DL. J Biomed Mater Res A. 2011; 99A:16. [PubMed: 21793193]
59. Hopkins AM, De Laporte L, Tortelli F, Spedden E, Staii C, Atherton TJ, Hubbell JA, Kaplan DL. Adv. Funct. Mater. 2013; 23:5140.
60. Rogers, W. Sterilisation techniques for polymers in Sterilisation of biomaterials and medical devices. In: Lerouge, S.; Simmons, A., editors. Woodhead Publishing; Sawston, Cambridge, UK: 2012. Ch.2
61. Kempner ES. J. Pharm. Sci. 2001; 90:1637. [PubMed: 11745722]

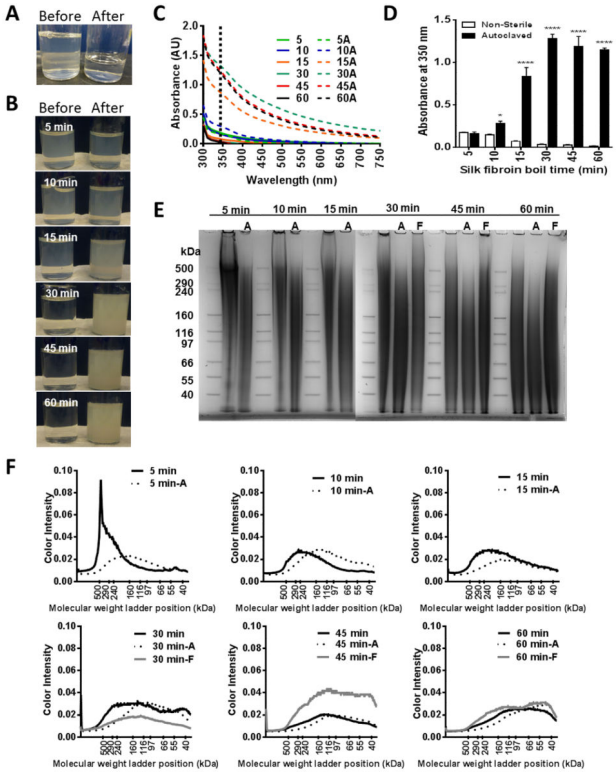

Figure 1.

Effects of silk fibroin solution sterilization upon silk fibroin protein. (A) A representative image of the silk fibroin solution before and after sterile filtration through a 0.22 μm syringe filter. (B) Representative images of the silk fibroin solution before and after autoclave sterilization, where time labels denote the silk fibroin boil time. (C) Absorbance spectra of the silk fibroin solutions boiled for 5-60 min before (5-60) and after autoclave sterilization (5A-60A). (D) Absorbance of the silk fibroin solutions at 350 nm. (E) SDS-PAGE of silk fibroin solutions before and after sterilization by either filtration (F) or autoclaving (A). n=3, ****$p<0.0001$, *$p<0.05$, compared to non-sterilized samples. (F) Protein fragment size distribution analysed from SDS-PAGE gels following either autoclaving (A) or filtration (F).

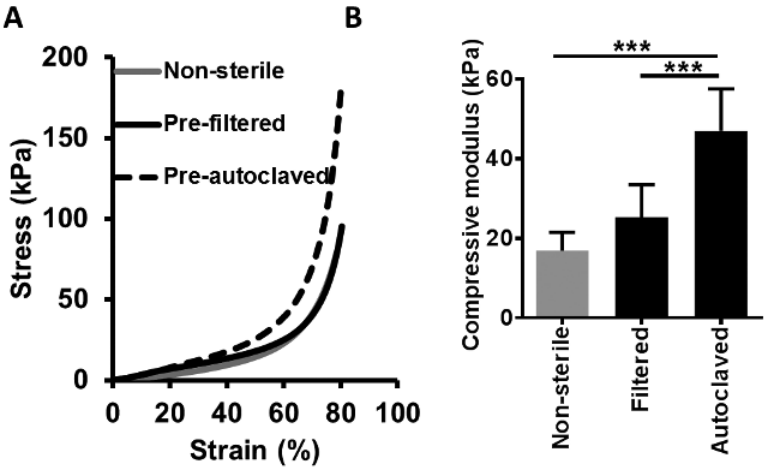

Figure 2.

Effects of silk fibroin solution sterilization upon the mechanical properties of the scaffold. (A) Stress-strain curve and (B) compressive modulus of silk fibroin scaffolds formed from non-sterilized silk fibroin compared to scaffolds formed with silk fibroin that has been sterilized by either filtration or autoclaving. Scaffolds were tested under compressive loading in physiological temperature and pH conditions (PBS, pH 7.4, 37°C). $n \geq 4$, *** $p<0.001$.

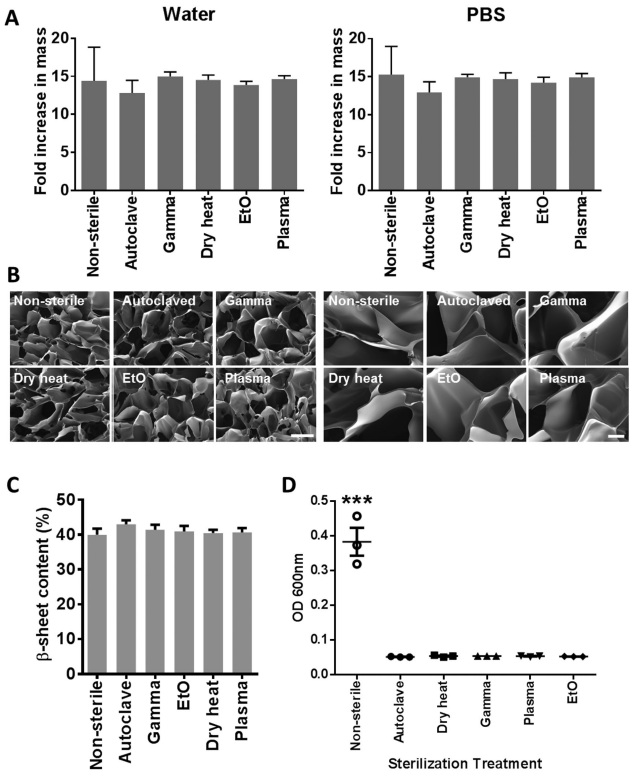

Figure 3.

Effects of silk fibroin scaffold sterilization upon the physical characteristics of the scaffold. (A) Silk fibroin scaffold swelling in water or PBS following sterilization expressed as fold increase in mass compared to dry scaffolds, n=5. (B) Representative scanning electron microscopy images of the silk fibroin scaffolds following sterilization. The scale bar for the images on the left = 200 μm and on the right = 40 μm. (C) FTIR spectra of sterilized silk fibroin scaffolds (D) β-sheet content of sterilized silk fibroin scaffolds determined from FTIR spectra, n=4. (E) Sterility of sterilized silk fibroin scaffolds tested as bacterial growth (OD 600 nm) in Luria broth over 48h. n=3, *** $p<0.001$, compared to all sterilized samples.

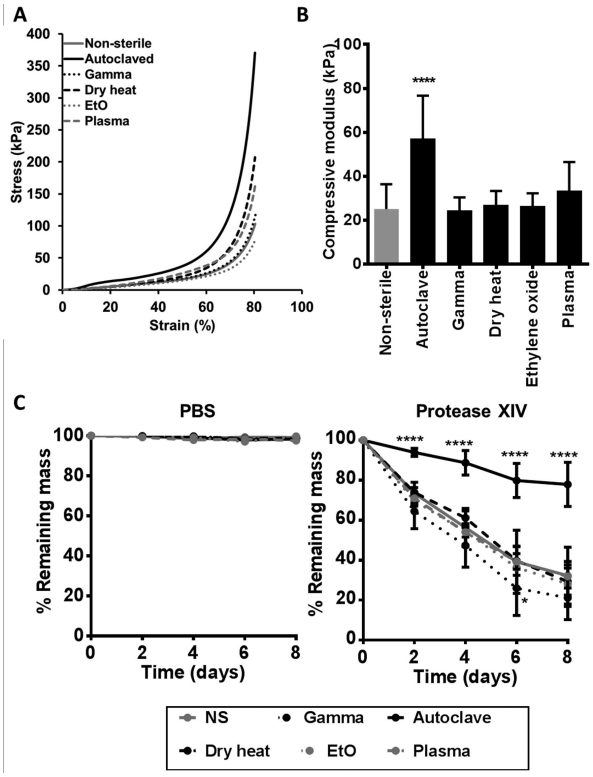

Figure 4.

Effects of silk fibroin scaffold sterilization upon the mechanical (A-B) and degradation (C) properties of the scaffold. (A) Stress-strain curve and (B) compressive modulus of sterilized silk fibroin scaffolds. Scaffolds were tested under compressive loading in physiological temperature and pH conditions (PBS, pH 7.4, 37°C). n≥16, **** $p<0.0001$, compared to non-sterilized sample. (C) Degradation of sterilized silk fibroin scaffolds in PBS or Protease XIV over an 8 day period at 37°C. Scaffold degradation is expressed at % remaining mass, where lower % remaining mass indicates more degradation. n=7, * $p<0.5$, **** $p<0.0001$, compared to non-sterilized samples.

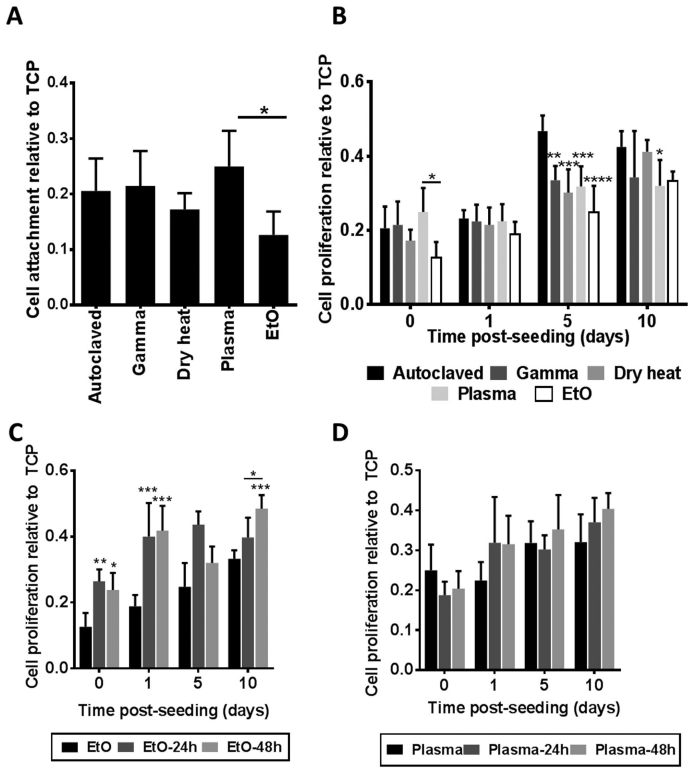

Figure 5.

Effects of silk fibroin scaffold sterilization upon cell attachment and proliferation. (A) Cell attachment after 3 h, n=5, * $p<0.05$. (B) Cell proliferation at 1, 5, and 10 days post seeding, n=8. p-values are calculated relative to the autoclaved samples (unless shown otherwise in the graph), * $p<0.05$, ** $p<0.01$, *** $p<0.001$, **** $p<0.0001$. (C) Cell proliferation on silk fibroin scaffolds sterilized with ethylene oxide following a 24 or 48 h incubation in PBS to leach out ethylene oxide prior to cell seeding, n=3, * $p<0.05$, ** $p<0.01$, *** $p<0.001$, compared to non-leached samples or as indicated in the figure. (D) Cell proliferation on silk fibroin scaffolds sterilized with H_2O_2 gas plasma following a 24 or 48 h incubation in PBS to leach out H_2O_2 prior to cell seeding, n=3 All attachment and proliferation measurements were obtained using the Alamar Blue assay.

Table 1

Summary of findings for the effect of different sterilization techniques on the properties of silk fibroin protein solution and lyophilized silk fibroin scaffolds.

	Technique	Sterilization conditions	Sterilization principle	Advantages	Disadvantages
Liquid silk fibroin	**Autoclaving**	High pressure saturated steam; 121°C, 20 min, liquid cycle	Coagulation of vital microbial proteins and cellular components	Readily available Non-cytotoxic Cost-effective	Changes physical properties of silk fibroin protein: ↓ MW, ↑ protein aggregation Alters mechanical properties of scaffolds formed from autoclaved silk fibroin
	Sterile filtration	0.22 μm sterile filter	Size exclusion of microbes	Readily available Non-cytotoxic Cost-effective	Only applicable to low viscosity silk fibroin solutions- ie. low MW, low concentration Losses in sample volume & sample concentration with ↑ MW and concentration
Silk fibroin scaffolds	**Autoclaving**	High pressure saturated steam; 121°C, 20 min, solid cycle	Coagulation of vital microbial proteins cellular components	Readily available Non-cytotoxic Cost-effective	Changes physical properties of silk fibroin scaffolds- ↓ degradation rate, ↑ compressive modulus Not applicable for silk fibroin scaffolds functionalized with biological molecules
	Gamma irradiation	Ionizing gamma rays 16.6×10^3 rad/min until 1.5 Mrad	Creation of free radicals that cause intracellular damage	Commonly used in hospitals & laboratories Non-cytotoxic	Not readily available Costly ↑ protein degradation rate Potential protein damage and cross-link formation
	Dry heat	High temperature 20 min, 160-170°C	Oxidation and coagulation of cellular components	Readily available Cost-effective	Not applicable for silk fibroin scaffolds functionalized with biological molecules
	Ethylene oxide (EtO)	EtO gas for 10 h at room temperature, 2 h degassing in the sterilizer chamber, 24 h degassing in a vacuum oven at room temperature	Alkylation reactions with cellular components	Commonly used to sterilize heat-sensitive materials and equipment	Not readily available Highly toxic ethylene oxide material, risk to users Cytotoxic- ↓ cell attachment and proliferation rate- can be improved by pre-leaching ethylene oxide out of silk fibroin scaffolds
	Hydrogen Peroxide (H_2O_2) gas plasma	H_2O_2 vaporized into the chamber followed by generation of gas plasma using the STERRAD sterilization system	Oxidation of cellular components	Commonly used in hospitals & laboratories Low-temperature technique	Not readily available

Table 2

Efficiency of silk fibroin solution sterilization. Percent recovery of the silk fibroin solution following sterile filtration through a 0.22 μm syringe filter. Time labels denote the silk fibroin boil time.

Conc. (wt%)	5 min	10 min	15 min	30 min	45 min	60 min
0.5	0	13.4 ± 2.6	15.2 ± 0.8	84.2 ± 3.8	n/a	n/a
1	0	0	6.9 ± 4.9	78.3 ± 9.5	n/a	n/a
2	0	0	3.7 ± 3.3	44.2 ± 3.8	n/a	n/a
4	0	0	0	27.7 ± 5.5	90.0 ± 6.6	95.0 ± 0.0

Table 3

Efficiency of silk fibroin solution sterilization. Percent concentration retention following sterilization of silk fibroin solution through a 0.22 μm syringe filter. Time labels denote the silk fibroin boil time.

Conc. (wt%)	5 min	10 min	15 min	30 min	45 min	60 min
0.5	0	89.0 ± 19.0	39.7 ± 33.5	98.4 ± 18.1	n/a	n/a
1	0	41.8 ± 21.4	56.9 ± 39.0	97.9 ± 14.0	n/a	n/a
2	0	0	74.2 ± 4.3	98.7 ± 1.0	n/a	n/a
4	0	0	0	97.3 ± 3.3	96.3 ± 3.7	102.6 ± 4.8